Available online at www.sciencedirect.com
ScienceDirect
Nuclear Physics B Proceedings Supplement 00 (2014) 1–3
Nuclear Physics B Proceedings Supplement

# Transverse energy-energy correlations at next-to-leading order in $\alpha_s$ at the LHC.

A. Ali[a], F. Barreiro[b], J. Llorente[b], W. Wang[c]

[a] *Deutsches Elektronen-Synchrotron DESY.*
[b] *Dpto. Física Teórica, Universidad Autónoma de Madrid.*
[c] *Helmholtz-Institut für Strahlen- und Kernphysik, Universität Bonn.*

**Abstract**

We compute the transverse energy-energy correlation (EEC) and its asymmetry (AEEC) at next-to-leading order (NLO) in $\alpha_s$ in $pp$ collisions at the LHC for the nominal center-of-mass energies of 7, 8 and 13 TeV. We show that the transverse EEC and the AEEC distributions have small sensitivity to the QCD factorisation and renormalisation scales and are almost insensitive to the structure functions of the proton. Hence, they can be used to precisely test QCD in hadron colliders and determine the strong coupling $\alpha_s$.

*Keywords:* QCD, jet, EEC

## 1. Definition of the observable

The transverse energy-energy correlation function (EEC) is defined as the energy-energy weighted differential cross-section in the azimuthal angles between pairs of jets [1].

$$\frac{1}{\sigma}\frac{d\Sigma^{\rm EEC}}{d\phi} \equiv \frac{1}{N}\sum_{k=1}^{N}\frac{1}{\Delta\phi}\sum_{(i,j)}\frac{E_{{\rm T}i}^{(k)}E_{{\rm T}j}^{(k)}}{\left(E_{\rm T}^{(k)}\right)^2} \qquad (1)$$

At leading order, it can be expressed as the ratio of the 3-jet differential cross section to the 2-jet integrated cross sections, which, by virtue of the factorsation theorem, are obtained from their respective convolutions with the parton density functions (PDF)

$$\frac{1}{\sigma}\frac{d\Sigma^{\rm EEC}}{d\phi} = \frac{\sum_{(i,j)} f_i(x_1)f_j(x_2)\otimes\hat{\Sigma}^{ij\to klm}}{\sum_{(i,j)} f_i(x_1)f_j(x_2)\otimes\hat{\sigma}^{ij\to kl}} \sim \frac{\alpha_s(\mu)}{\pi}F(\phi) \qquad (2)$$

At next-to-leading order (NLO) in $\alpha_s$, its perturbative expansion can be expressed as

$$\frac{1}{\sigma}\frac{d\Sigma^{\rm EEC}}{d\phi} \sim \frac{\alpha_s(\mu)}{\pi}F(\phi)\left[1+\frac{\alpha_s(\mu)}{\pi}G(\phi)\right] \qquad (3)$$

with $F(\phi)$ and $G(\phi)$ appropriate functions of the azimuthal angle. It is also useful to define the EEC forward-backward asymmetry (AEEC) as

$$\frac{1}{\sigma}\frac{d\Sigma^{\rm AEEC}}{d\phi} = \frac{1}{\sigma}\frac{d\Sigma^{\rm EEC}}{d\phi}\bigg|_{\pi-\phi} - \frac{1}{\sigma}\frac{d\Sigma^{\rm EEC}}{d\phi}\bigg|_{\phi} \qquad (4)$$

The AEEC is convenient as it cancels out further corrections from hadronisation and other non-perturbative effects such as multiparton interactions, ubiquous in an experimental $pp$ collision environment.

## 2. Properties

It has been shown in [1], that these observables have a large sensitivity to the strong coupling constant $\alpha_s(m_Z)$, and only a small sensitivity to the QCD renormalisation and factorisation scales $\mu_R$ and $\mu_F$. Also, as it is a ratio, the contributions from the uncertainties on the parton density functions (PDF) are cancelled out to a very large extent.
It is also expected that, due to the energy-energy weighting in Eq. 1, the experimental uncertainties arising from the jet calibration and calorimetric resolution are also cancelled out, thus providing high sensitivity for the extraction of $\alpha_s$.

## 3. Kinematical selection

For this study, $pp$ collision events have been simulated using NLOJET++ [2] coupled to the MSTW parton distribution functions [3]. The renormalisation and factorisation scales are taken to be the mean value of the transverse momenta for the two leading jets. $\mu_R = \mu_F = \langle p_{T12} \rangle$. Jets have been reconstructed from the outcoming partons using the anti-$k_t$ algorithm as implemented in FastJet [4], with radius parameter $R = 0.4$. We require at least two jets with $p_T > p_T^{\min}$ and $|\eta| < 2.5$. In addition the two leading jets have to fulfill $p_{T1} + p_{T2} > 500$ GeV.

## 4. Dependence on the strong coupling $\alpha_s$

In this section, the dependence of the EEC and AEEC on the strong coupling constant $\alpha_s$ is investigated. To this end, the EEC and AEEC distributions are obtained for the values of $\alpha_s = 0.107, 0.117$ and $0.127$, provided in the MSTW parton density fits. The results for these three values are shown in Fig. 1 As it can be seen in Fig.

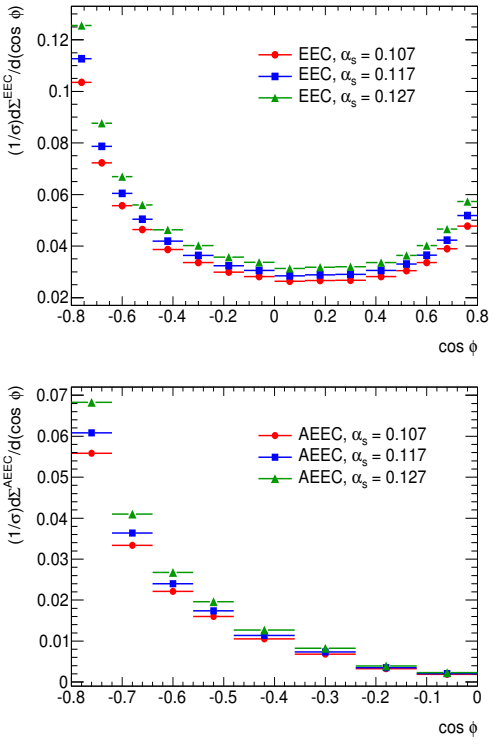


Figure 1: The EEC (top) and AEEC (bottom) distributions for three values of the strong coupling constant $\alpha_S$.

1, a larger value of $\alpha_s$ gives larger values for the central plateau in the EEC distributions. This means that the high $p_T$, large angle radiative activity is enhanced. For the AEEC a similar effect is also seen.

## 5. Dependence on $p_T^{\min}$ and $\sqrt{s}$

In this section, the dependence of the observables with $p_T^{\min}$ at fixed $\sqrt{s}$, with $\sqrt{s}$ at fixed $p_T^{\min}$ and $\sqrt{s}$ at fixed $x_T^{\min}$ is investigated. Here $x_T^{\min}$ is defined as $p_T^{\min} / \sqrt{s}$

### 5.1. Dependence on $p_T^{\min}$

The EEC and AEEC distributions also present a dependence on the minimum transverse momenta of the subleading jets. This is understood to be due to the fact that, for lower thresholds, the amount of uncorrelated activity is significantly increased, as illustrated in Figure 2 for both the EEC and AEEC.

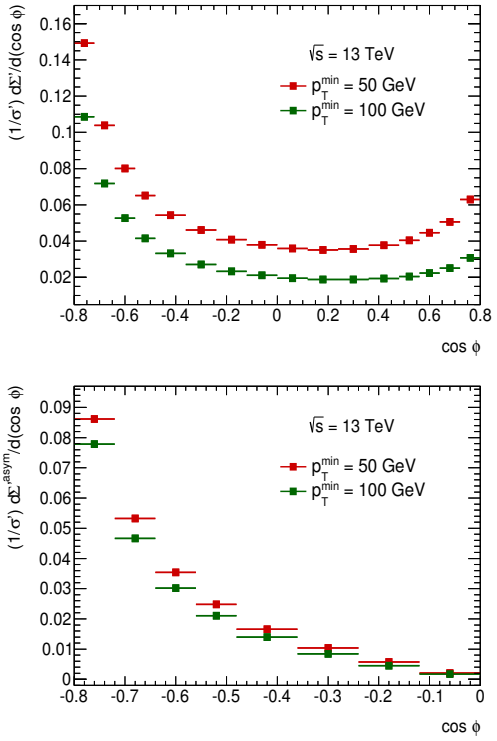


Figure 2: The dependence of the EEC (top) and AEEC (bottom) distributions on the minimum jet transverse momenta $p_T^{\min}$.

### 5.2. Dependence on $\sqrt{s}$

The dependence of the EEC and AEEC on the center-of-mass energy $\sqrt{s}$ is investigated. The bin-by-bin dependence on $\sqrt{s}$ is expected to follow a logarithmic law of the form $\phi_i(\sqrt{s}) = A_i \log(\sqrt{s}) + B_i$, with $A_i$ and $B_i$ appropriate constants, for both the EEC and its asymmetry. The results are shown in Fig. 3.

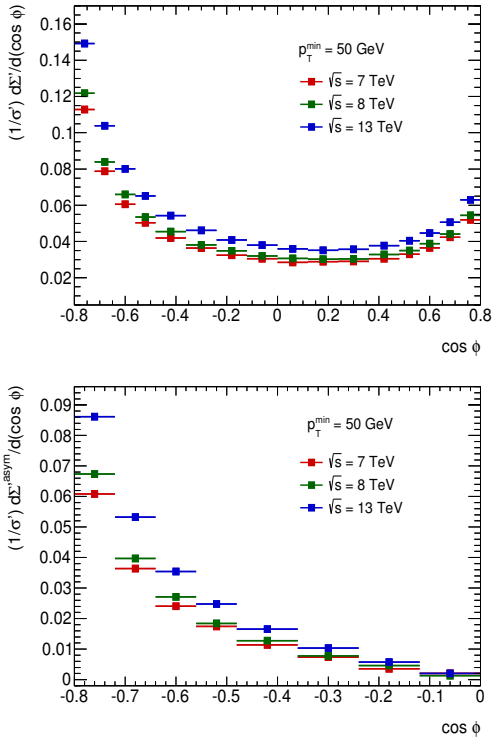


Figure 3: The dependence of the EEC (top) and AEEC (bottom) distributions on the proton-proton center-of-mass energy $\sqrt{s}$.

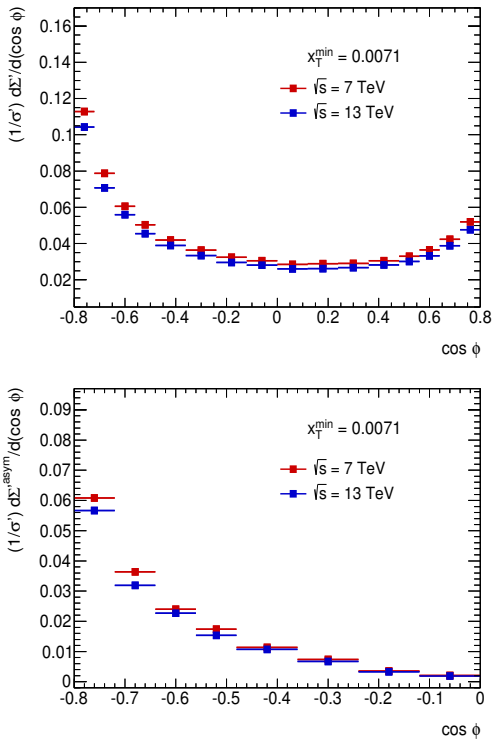


Figure 4: The dependence of the EEC (top) and AEEC (bottom) distributions on $\sqrt{s}$ at fixed $x_{\mathrm{T}}^{\mathrm{min}}$ and $x_{\mathrm{T1}} + x_{\mathrm{T2}}$.

### 5.3. *Dependence on $\sqrt{s}$ at fixed $x_{\mathrm{T}}^{\mathrm{min}}$*

Here, we look for a scale invariant behaviour of the EEC and AEEC by comparing the EEC and AEEC at $\sqrt{s} = 7, 13$ TeV for fixed values of $x_{\mathrm{T}}^{\mathrm{min}} = p_{\mathrm{T}}^{\mathrm{min}}/\sqrt{s} = 50/7000$ and $x_{\mathrm{T1}} + x_{\mathrm{T2}} = (p_{\mathrm{T1}} + p_{\mathrm{T2}})/\sqrt{s} = 500/7000$. This is shown in Fig. 4

## 6. Theoretical uncertainties

The main theoretical uncertainties for this observable are the scale dependence and the PDF uncertainty. The scale dependence is investigated by shifting up and down independently the renormalisation and factorisation scales $\mu_R$ and $\mu_F$ by a factor of two. The maximal envelope of the differences is taken to be the nominal scale uncertainty, which can amount up to 10% for the EEC and 5% for the AEEC (see Fig. 5). For the PDF uncertainty, the MSTW eigenvectors at 68% CL are used, and the differences are added in quadrature. The total PDF uncertainty is smaller than 1%, as shown in Fig. 5.

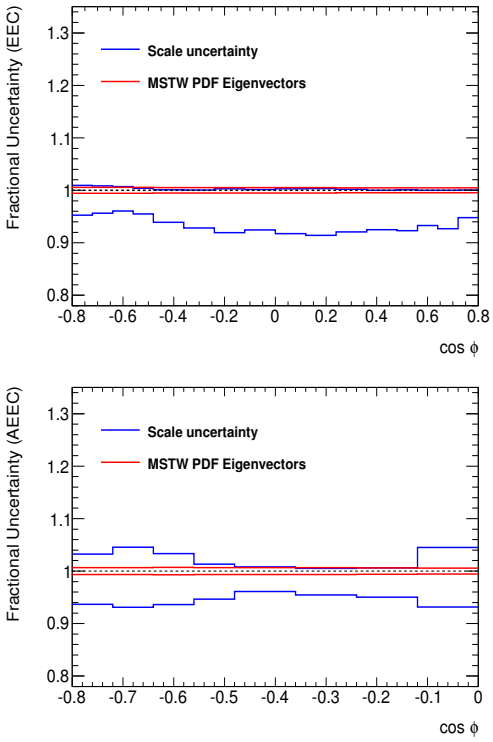


Figure 5: Theoretical uncertainties for the EEC (top) and AEEC (bottom) arising from the scale ambiguities and the parton densities.

[1] A. Ali *et al.* [Phys. Rev. D **86**, 114017 (2012)].
[2] Z. Nagy, [Phys. Rev. Lett. **88**, 122003 (2002)].
[3] A.D. Martin *et al.* [Eur. Phys. J. **C63**, 189-285 (2009)]
[4] M. Cacciari *et al.* [Eur. Phys. J. **C72** 1896 (2012)].